

Adenosine triphosphatase pontin is overexpressed in hepatocellular carcinoma and coregulated with reptin through a new posttranslational mechanism

Valérie Haurie ¹ valerie.haurie@inserm.fr , Ludovic Ménard ¹ ludome@gmail.com , Alexandra Nicou ¹ alexandranicou@yahoo.fr , Christian Touriol ² Christian.touriol@inserm.fr , Philippe Metzler ¹ metzlerphilippe@hotmail.com , Jérémy Fernandez ¹ j.fernandez40@yahoo.fr , Danièle Taras ¹ Daniele.Taras@inserm.fr , Patrick Lestienne ¹ Patrick.lestienne@inserm.fr , Charles Balabaud ^{3,1} charles.balabaud@chu-bordeaux.fr , Paulette Bioulac-Sage ^{1,4} paulette.bioulac-sage@gref.u-bordeaux2.fr , Hervé Prats ² herve.prats@inserm.fr , Jessica Zucman-Rossi ⁵ jessica@inserm-U674.net , Jean Rosenbaum ^{1*} jean.rosenbaum@gref.u-bordeaux2.fr

¹ Fibrose hépatique et cancer du foie INSERM : U889 , Université Victor Segalen - Bordeaux II , IFR66 , 146 rue léo saignat, 33076 Bordeaux Cedex,FR

² I2MR, Institut de médecine moléculaire de Rangueil INSERM : U858 , IFR31 , IFR150 , Université Paul Sabatier - Toulouse III , Institut Louis Bugnard 1, avenue Jean Poulhes BP 84225 31432 TOULOUSE CEDEX 4,FR

³ Service d'hépatogastroentérologie CHU Bordeaux , FR

⁴ Laboratoire d'anatomie pathologique CHU Bordeaux , Groupe hospitalier Pellegrin , FR

⁵ Genomique Fonctionnelle des Tumeurs Solides INSERM : U674 , Université Paris-Diderot - Paris VII , IFR105 , Hopital Saint-Louis - IFR 105 PARIS VII 27, Rue Juliette Dodu 75010 PARIS,FR

* Correspondence should be adressed to: Jean Rosenbaum <jean.rosenbaum@gref.u-bordeaux2.fr >

Abstract

Reptin and Pontin are related ATPases associated in stoichiometric amounts in several complexes involved in chromatin remodeling, transcriptional regulation and telomerase activity. We found that Reptin was upregulated in hepatocellular carcinoma (HCC) and that down-regulation of Reptin led to growth arrest. We show here that Pontin mRNA is also upregulated in human HCC 3.9 fold as compared to non-tumor liver (p = 0.0004). Pontin expression was a strong independent factor of poor prognosis in a multivariate analysis. As for Reptin, depletion of Pontin in HuH7 cells with siRNAs led to growth arrest. Remarkably, Pontin depletion led to down-regulation of Reptin as shown with Western blot, and conversely. Whereas siRNAs induced a decrease of their cognate mRNA targets, they did not affect the transcripts of the partner protein. Translation of Pontin or Reptin was not altered when the partner protein was silenced. However, pulse-chase experiments demonstrated that newly synthesized Pontin or Reptin stability was reduced in Reptin or Pontin depleted cells; respectively. This phenomenon was reverted upon inhibition of proteasome or ubiquitin-activating enzyme (E1). In addition, proteasome inhibition could partly restore Pontin steady-state levels in Reptin-depleted cells, as shown by Western blot. This restoration was no more observed when cells were also treated with cycloheximide, thus confirming that proteasomal degradation in this setting was restricted to newly synthesized Pontin. Conclusion: Reptin and Pontin protein levels are strictly controlled by a post-translational mechanism involving proteasomal degradation of newly synthesized proteins. These data demonstrate a tight regulatory and reciprocal interaction between Reptin and Pontin, which may in turn lead to the maintenance of their 1:1 stoichiometry.

MESH Keywords Apoptosis ; Carcinoma, Hepatocellular ; pathology ; Carrier Proteins ; genetics ; physiology ; Cell Proliferation ; DNA Helicases ; genetics ; physiology ; Humans ; Liver Neoplasms ; pathology ; Proteasome Endopeptidase Complex ; antagonists & inhibitors ; Protein Biosynthesis ; RNA, Messenger ; analysis

Author Keywords proteasome ; ubiquitin ; translation ; helicase ; prognosis

Hepatocellular carcinoma (HCC) is the main type of primary liver cancer. It is the fifth most common cancer worldwide and bears a very poor prognosis, mainly because of the lack of efficient therapy. Looking for new targets, we performed a comparative proteomic analysis between HCC and peri-tumoral liver, which led to the discovery of many deregulated proteins (1), including Reptin. Reptin overexpression was associated with a poor prognosis, and we demonstrated that Reptin was required for HCC cell viability and growth, and that Reptin overexpression conferred a greater ability to tumor cells for growth in xenografts (2).

Reptin (TIP48, TIP49b, RuvBL2, TAP54 β , ECP-51) and Pontin (or TIP49, RuvBL1, TAP54 α , ECP-54) are closely-related members of the AAA+ family of ATPases (ATPases Associated with various cellular Activities (3)) that show remarkable conservation from yeast to human. Due to their participation in several distinct multi-protein complexes (reviewed in (4, 5)), they are involved in chromatin remodeling (6–8), transcriptional regulation (6, 9, 10), DNA damage repair (7, 11), snoRNA biogenesis (12) and telomerase activity (13). Because Reptin is usually associated with Pontin in complexes where they are present in stoichiometric amounts (7, 8, 10, 14–19), we studied Pontin expression and function in HCC. We found that Pontin was also up-regulated in HCC and unexpectedly that Pontin and Reptin expression was co-regulated via a novel post-translational mechanism.

Experimental procedures

Liver samples and real-time RT-PCR

Samples came from resected or explanted livers with HCC of patients treated in Bordeaux from 1992 to 2005. Fragments of fresh tumor and non-tumor liver tissues (taken at a distance of at least 2 cm from the tumor) were either snap-frozen in liquid nitrogen and stored at -80°C , or fixed with formalin and embedded in paraffin. 104 HCC samples (supporting Table 1) were used for real-time RT-PCR analysis. 18 non-tumor liver samples were used as a control group. RNA extraction and real-time RT-PCR were performed as described (2 , 20). Pre-developed sequence detection reagents specific for human RUVBL1 gene (Applied Biosystems, Courtaboeuf, France) were used as described (20) using the $2^{-\Delta\Delta\text{CT}}$ method (21). Gene expression results were normalized to internal control ribosomal 18S.

Immunohistochemistry

This was done as described (2) using a mouse monoclonal Pontin antibody (22) diluted to $1.6\ \mu\text{g}/\mu\text{l}$.

Transient transfection of small interfering RNA (siRNA)

We used two targeting siRNAs for each Reptin (R1 and R2 (2)) and Pontin mRNAs (P1 and P2, Supporting Table 2). Controls were either scrambled R2 and P2 sequences, or the GL2 siRNA targeting Firefly luciferase (MWG, Ebersberg, Germany). siRNAs were transfected at a concentration of 125nM with Lipofectamine (Invitrogen, Cergy Pontoise, France).

Cell proliferation assay and caspase 3 activity measurement

Cells were counted with a Coulter counter (Beckman Coulter, Villepinte, France) in duplicate wells. DNA synthesis was measured by the quantification of bromodeoxyuridine (BrdU) incorporation, and caspase 3 activity with a colorimetric assay (2).

Western blot

Cell extracts were prepared in RIPA buffer (23). We used Reptin, β -catenin (BD Biosciences, Pharmingen, Le Pont de Caix, France), FLAG-M2, β -actin (Sigma-Aldrich, Saint-Quentin Fallavier, France) mouse monoclonal, and Pontin rabbit polyclonal (ProteinTech, Chicago, IL) antibodies. Primary antibodies were detected by horseradish peroxidase conjugated, or infrared dye-labeled secondary antibodies (LI-COR, Lincoln, NE). Detection was achieved with the ECL kit (GE Healthcare, Saclay, France) or the Odyssey IR imaging system (LICOR), respectively.

Polyribosome fractionation

KGL2 and KR2 cells lines stably expressing an shRNA targeting Firefly luciferase or Reptin, respectively, in a doxycycline-dependent manner (Supporting Methods), were cultured with or without doxycycline. Cycloheximide ($100\ \mu\text{M}$) was added ten minutes before cell lysis. Sucrose-gradient fractionation and polysome-associated RNA purification were as described (24). RNAs were analyzed by cDNA synthesis and PCR amplification.

Metabolic labeling and immunoprecipitation

KGL2 and KR2 cells were stably transduced with a lentiviral vector coding HA-Pontin resulting in KGL2-HAP and KR2-HAP cell lines (Supporting Methods). Similarly, KP2 cells expressing the P2 Pontin shRNA (Supporting Methods), were transduced with Flag-Reptin (2), resulting in KP2-FR cells. Cells were incubated in Methionine/Cysteine-free medium for 30 min before pulse labeling with $150\ \mu\text{Ci}/\text{ml}$ EXPRE³⁵ S³⁵ S Protein Labeling Mix (Perkin Elmer, Courtaboeuf, France) for 15 min at 37°C . Cells were washed then scraped in lysis buffer ($50\ \text{mM}$ Tris-HCl pH 7.5, $150\ \text{mM}$ NaCl, $4\ \text{mM}$ EDTA, 1% Triton, 1% SDS) supplemented with protease inhibitor cocktail (Roche, Meylan, France). The amount of radiolabeled TCA-precipitated material was measured by scintillation counting.

For pulse-chase experiments, cells were labeled with $100\ \mu\text{Ci}/\text{mL}$ EXPRE³⁵ S³⁵ S Protein Labeling Mix for 1h, washed with medium supplemented with $2\ \text{mM}$ cysteine/methionine, and cultured for various times in this chase medium supplemented with the indicated agents before harvesting.

Cell extracts were diluted in lysis buffer without SDS and incubated for 2 hours at 4°C with monoclonal anti-HA-Agarose or anti-Flag M2 beads (Sigma-Aldrich). The beads were washed 5 times with lysis buffer and eluted with Laemmli sample buffer. Eluates were separated on a 10% SDS-PAGE. In some cases, Pontin was precipitated with a polyclonal anti-Pontin antibody.

Signals from radiolabeled protein bands were acquired in an Instant-Imager (Packard, Perkin-Elmer). Protein degradation rate is expressed as half-life ($t_{1/2}$), the time where 50% of the protein is degraded. The results are expressed as mean \pm SEM of five to six independent determinations.

Statistical analysis

Statistical analyses were performed using the 2-tailed Student t test, or 1-way analysis of variance (ANOVA) when comparing multiple means. Statistical significance was set at a p value of less than 0.05. Correlations between mRNA levels of expression and qualitative variables were calculated with the non-parametric Kruskal-Wallis test with STATA software (Stata Corp., College Station, TX). The ages of patients and diameters of the tumors were partitioned with a median. For survival analysis, expression data were logarithm 10-transformed and dichotomized according to the median. Survival comparisons were done by log-rank test. Survival curves were obtained by the Kaplan-Meier method. Multivariate analyses were performed using Cox model. All survival analyses were performed using STATA software 8.2.

Results

Pontin is overexpressed in human HCC

There was a 3.9-fold increase in Pontin transcripts in HCC as compared to non-tumor livers (Fig. 1A, $p < 0.0004$). Pontin mRNA levels were highly correlated with those of Reptin mRNA ($r^2 = 0.78$, $p < 0.0001$, Fig. 1B). Immunohistochemistry confirmed the overexpression of Pontin in HCC with the same pattern as Reptin, and showed that, similar to Reptin (2), Pontin was partly localized to the cytoplasm of tumor cells (Fig. 1C–E). Pontin mRNA levels were correlated with features of poor prognosis: levels were higher in large tumors (> 60 mm, $p = 0.026$), in tumors with vascular embolism ($p = 0.047$), portal invasion ($p = 0.008$), or chromosomal instability (fractional allelic loss > 0.128 , $p = 0.02$), in patients with early relapse following curative surgery ($p = 0.001$) or who died within 3 years of surgery ($p = 0.001$). A significant shorter disease-free survival in patients with high Pontin level was observed as compared to those with low level (Fig. 1F, $p = 0.0022$). Most importantly, using a Cox model multivariate analysis, high Pontin mRNA levels remained associated with shorter disease-free survival after adjustment for age, gender, tumor diameter and the presence of vascular embolism (Hazard Ratio = 3.9, 95% CI = [1.9–8.0], $p = 0.003$).

Pontin silencing reduced cell proliferation and induced apoptosis

Pontin mRNA level was significantly reduced with P1 ($70\% \pm 13\%$) and P2 ($77\% \pm 12\%$) siRNAs (Fig. 2A). The siRNAs also greatly decreased Pontin protein expression ($78.6\% \pm 6.9\%$ with P1 and $87.7\% \pm 9.0\%$ with P2) (Fig. 2B).

Starting from Day 3 after transfection, the growth of cells transfected with Pontin siRNAs strikingly decreased (Fig. 2C). This was associated with both reduced DNA synthesis, evidenced by decreased BrdU incorporation, and increased apoptosis, demonstrated by an increased caspase 3 activity (Fig. 2D).

Concomitant down-regulation of Reptin and Pontin

Because findings with Pontin silencing were reminiscent of those we obtained previously upon Reptin silencing, we evaluated Reptin expression after transfection of Pontin siRNAs. Surprisingly, Reptin protein level was markedly reduced after transfection of P1 or P2 compared to control siRNA. The reciprocal observation was done in cells transfected with the Reptin-specific R1 and R2 siRNAs where Pontin protein level was also decreased (Fig. 3A–B). Because of the significant homology between Reptin and Pontin, we performed extensive control experiments that allowed excluding cross-reactivity of antibodies (Supporting Fig. 1).

To rule out off-target effects of siRNAs, we used a rescue strategy. Cell lines resistant to siRNAs were established by transduction of lentiviral vectors bearing either HA-Pontin or Flag-Reptin cDNA in which silent mutations have been introduced in the sequence targeted by the P2 or R2 siRNAs (Supporting Fig. 2). Reptin protein expression was no more decreased by P2 siRNA in P2-resistant cells, whereas it was reduced as expected upon transfection of P1 siRNA (Fig. 3C). Similarly, Pontin expression was not affected in cells expressing FLAG-Reptin resistant to the R2 siRNA (Fig. 3D). Altogether, these results showed that the down-regulation of Pontin was a direct consequence of the silencing of Reptin and reciprocally.

We then asked if our findings were specific of HuH7 cells. We examined the consequences of Reptin or Pontin silencing in another human liver cell line (HepG2), in human breast cancer cells (MCF7), in human prostatic cancer cells (LNCap) and in HeLa cells. We also tested the co-extinction of Pontin after transfection of the R2 siRNA in mouse (Hepa 1–6) or rat hepatoma cells (FAO). In every case, we observed a concomitant reduction of Reptin and Pontin protein levels (Supporting Fig. 3). These results argued in favor of a general rather than a cell-specific process for regulation of Pontin and Reptin expression.

Reptin silencing does not decrease Pontin mRNA level (and reciprocally)

Reptin and Pontin interact with transcription factors and bind to gene promoters (reviewed in (4)). We thus hypothesized that they could regulate reciprocally their expression through a transcriptional mechanism. However, transfection of Pontin siRNAs did not alter Reptin mRNA levels, whereas as expected, Pontin mRNA decreased. Reciprocally, Reptin, but not Pontin mRNA levels were efficiently silenced with Reptin siRNAs (Fig. 4A–B).

As an additional control, we tested whether Reptin produced from an mRNA devoid of its natural regulatory sequences would also be depleted upon transfection of a Pontin siRNA. We used HuH7 cells stably expressing N-term FLAG-tagged Reptin from the viral MND promoter (2). We found that the level of both endogenous and Flag-tagged Reptin was decreased after transfection of Pontin specific siRNAs (Supporting Fig. 4A). We obtained similar results with HeLa cells expressing FLAG/HA-tagged Reptin or Pontin from the CMV promoter (Supporting Fig. 4B).

Altogether, these experiments allow concluding that the reduction of Reptin or Pontin protein levels upon silencing of the respective binding partner is not related to a transcriptional effect, and thus occurs by a post-transcriptional mechanism.

Reptin silencing does not alter Pontin mRNA translation (and reciprocally)

Given the pleiotropic role of Reptin and Pontin, we hypothesized that they might regulate their partner's translation. This was tested using polyribosome fractionation and RT-PCR analysis in HuH7 cell lines stably expressing shRNAs targeting either Firefly luciferase (KGL2) or Reptin (KR2), in a doxycycline-dependent manner (Supporting Fig. 5). The polysomal distribution of Pontin mRNA was analyzed after 4 days of culture with or without doxycycline (Fig. 5A–B). In KGL2 cells, Reptin and Pontin transcripts exhibited a similar profile and were found all along the gradient, with an enhancement in the heaviest fractions, associated with polyribosomes. As expected, in doxycycline-treated KR2 cells, Reptin mRNA became barely detectable, whereas the profile of Pontin mRNA was unchanged as compared to that in KGL2 cells, and its distribution over the fractions was similar to the profile of GAPDH mRNA. When cells were incubated with puromycin for one hour prior to extraction, the profile of Pontin and GAPDH mRNAs shifted from heavy fractions to the top of the gradient (Fig. 5B). Because puromycin is a polypeptide chain terminator that causes premature termination of translation, our results demonstrate a genuine association of Pontin mRNA with polyribosomes, even in conditions where Reptin is depleted.

To make sure that Pontin mRNA was indeed actively translated, we performed metabolic labeling after 4 days of culture with doxycycline using cells stably expressing HA-Pontin (KGL2-HAP and KR2-HAP). After a 15 min pulse of radiolabeled methionine/cysteine, the level of ³⁵S incorporation into newly synthesized proteins was not different between KGL2-HAP and KR2-HAP cells (78.8% ± 4.3% vs 71.6 ± 6.8%, respectively), suggesting no gross alteration in overall protein biosynthesis in Reptin silencing conditions. After immunoprecipitation with anti-HA antibodies, the label accumulated in a 55-kDa band confirmed to be the full-length HA-Pontin polypeptide since it was reactive with an antibody against Pontin (Fig. 5C). When Reptin shRNA expression was induced in KR2-HAP cells, the amount of labeled HA-Pontin immunoprecipitated after a 15 min pulse was 98% of the control. This experiment showed that the decrease in HA-Pontin expression in cells expressing Reptin shRNA was not the consequence of a defective translation. Therefore, the association of Pontin mRNA with polyribosomes and the completion of HA-Pontin translation argued in favor of a post-translational regulation that explains the co-depletion of Pontin and Reptin. In reciprocal experiments, we also found that Pontin silencing did not alter Reptin translation, although Reptin silencing with R1 siRNA did reduce Reptin translation as expected (Fig. 5D).

Reptin silencing induces Pontin destabilization

Because Pontin and Reptin form a stoichiometric complex, we hypothesized that down-regulation of one of the two partners could disturb this stoichiometry and lead to post-translational destabilization of the binding partner. We thus measured Pontin half-life using metabolic labeling-chase experiments. Newly synthesized HA-Pontin was less stable upon Reptin silencing as shown by a significantly reduced half-life as compared to control ($t_{1/2} = 66.6 \pm 7.6$ vs 118 ± 21 min, $p = 0.002$) (Fig. 6A, 6C). Because the proteasome is the major intracellular proteolytic machinery in higher eukaryotic cells, we tested its involvement using specific inhibitors. Fig. 6B–C shows that MG132 was able to prolong the half-life of HA-Pontin in both Reptin-repleted and depleted conditions. The effect of Reptin depletion was specific since it did not alter the half-life of calnexin tested as a control (Fig. 6D).

We then asked if proteasome inhibitors could restore Pontin steady-state level in Reptin-depleted cells. We performed many experiments using a variety of experimental settings. For instance, Fig. 7A shows an experiment where, three days after induction of Reptin shRNA expression, HuH7 cells were treated with MG132 or epoxomycin for 4h. This did not modify the co-depletion although effective inhibition of the proteasome was confirmed by the accumulation of higher molecular weight forms of β -catenin, a proteasome target (25). Similar results were seen when using other MG132 concentrations, duration of treatment, or with other inhibitors such as clasto-Lactacystin- β -lactone (not shown). We hypothesized that if the stabilizing effect of proteasome inhibition was restricted to newly synthesized protein chains, our experiments might not be sensitive enough to detect an accumulation of proteins within the short time course of the experiments. We thus repeated them using HuH7 cells that stably express HA-Pontin. These cells have high levels of Pontin mRNA (not shown), and interestingly a higher rate of Pontin translation than control cells (Fig. 7B). They do however overexpress very little Pontin at the protein level, reminiscent of our previous results with Flag-Reptin (2) (Fig. 7B). When these cells were treated with MG132 for 4 hours, we could detect a significant increase in Pontin protein levels both in basal conditions and when Reptin was previously depleted upon shRNA induction with doxycycline (Fig. 7C–D). On the other hand, the low level of Reptin consecutive to R2 shRNA induction in doxycycline-treated cells was not increased by MG132. Similar results were obtained when the proteasome was inhibited with 2.5 μ M epoxomycin (not shown).

Altogether, these results suggested that the restoration seen with proteasome inhibition was restricted to the pool of freshly translated protein. This hypothesis was tested in experiments where, following Reptin depletion, proteasome inhibition with MG1342 or epoxomycin was done in the absence or in the presence of cycloheximide that blocks new protein synthesis. As shown in Fig. 7E-F, cycloheximide treatment prevented the restoration of Pontin levels in these conditions.

Since in most cases proteins are targeted to the proteasome following poly-ubiquitylation, we examined the stability of newly synthesized Pontin in the presence of the ubiquitin activating enzyme inhibitor UBEI-41 (Biogenova). We found indeed that newly synthesized Pontin stability was enhanced in cells with Reptin depletion when they were treated with UBEI-41 (Fig. 8A). We also performed the reverse experiment. We first showed that the stability of newly synthesized Reptin was reduced upon Pontin silencing (Fig. 8D, compare lanes 2 and 6), an effect reverted in great part by proteasome inhibition (Fig. 8D). Furthermore, Reptin stability in Pontin-depleted cells was also largely restored following inhibition of ubiquitin activating enzyme (Fig. 8D). These data proved that an ubiquitylation step was involved in the destabilization of Pontin and Reptin in this setting.

We next attempted to detect whether Pontin and Reptin underwent polyubiquitylation upon silencing of their partner. Because endogenous ubiquitin might be limiting, and in order to maximize the sensitivity of detection, we transduced KR2 cells with adenoviral vectors (kindly provided by H. Wodrich, Bordeaux) expressing either HA-ubiquitin and GFP, or GFP alone. After 3 days with or without Dox, the proteasome was inhibited with epoxomycin in order to allow accumulation of ubiquitylated proteins, and ubiquitin was precipitated using the HA tag. Western blot with a Pontin antibody failed to reveal ubiquitylated Pontin whereas ubiquitylated β -catenin was indeed detected (Supporting Fig. 6A). The same results were obtained when looking for Reptin ubiquitylation in KP2-FR cells (Supporting Fig. 6B).

Discussion

We show that Pontin is overexpressed in a large series of human HCC. High levels of Pontin mRNA were associated with features of poor prognosis. Using a multivariate analysis, we even found that Pontin level was an independent factor of poor prognosis when taking into account other poor prognosis factors including the presence of vascular embolism. In addition, *in vitro* experiments showed that Pontin was required for HCC cell growth and viability. All these findings, also including the cytoplasmic localization of Pontin in tumor cells, are highly reminiscent of those that we obtained with Reptin (2) and are in keeping with the known association of Pontin with Reptin into functional complexes (4, 5).

Surprisingly, silencing experiments led to a similar co-depletion of Pontin and Reptin, as recently found in HeLa cells (13). Our results were extended to a series of human cells from liver and non-liver origin and to other species, suggesting that co-depletion of Reptin and Pontin is a general finding. We demonstrate that Pontin and Reptin co-depletion is linked to a post-translational regulation since no changes in mRNA levels nor in translation were observed following silencing. On the other hand, we show that the stability of newly synthesized Pontin is reduced when Reptin is previously depleted, and reciprocally. This defect can be reverted when using a proteasome inhibitor. In addition, we show that proteasome inhibition is able to increase Pontin steady-state level whether Reptin levels are high or low. Proteasome inhibition had on the other hand no effect on the residual low levels of Reptin consecutive to RNAi. Together with our results with cycloheximide, this suggests that the restoration of Pontin levels due to proteasome inhibition is mainly the consequence of stabilization of newly translated Pontin, whereas no effect is seen for Reptin which translation is impaired because of RNAi. We suggest that Pontin and Reptin heteromers are formed immediately upon completion of translation, likely co-translationally. In that case, in the absence of its partner, newly translated Pontin or Reptin cannot be correctly folded and is targeted for proteasomal degradation. This is also in agreement with our data showing that Reptin and Pontin depletion follow identical kinetics upon use of any siRNA (Supporting Fig. 7). It is also possible that Pontin and Reptin act as chaperones for each other. A chaperone role can be inferred from their presence in a HSP90 complex conserved in human and yeast (26, 27), their role in the assembly of the Ino80 complex in yeast (28), and is coherent with the fact that many other members of the AAA+ family are indeed bona fide chaperones (3). In most cases, proteins undergo proteasome degradation following prior polyubiquitylation. Polyubiquitylation involves an ordered set of reactions beginning with activation of ubiquitin by the ubiquitin-activating enzyme E1 (29). We thus used an E1 inhibitor and found that the stability of both Pontin and Reptin was enhanced. We were however unable to directly detect polyubiquitylation of any of them even when ubiquitin was greatly overexpressed and proteasome inhibited. It may be that the sensitivity of ubiquitylation detection is still insufficient or that there is an intermediary protein that is ubiquitylated and regulates Pontin and Reptin turnover (30). Further experiments are needed to clarify this point.

Besides the co-depletion, results from our study also shed light on our previous observation that transduction of cells with a lentiviral vector coding Flag-tagged Reptin induced very little protein overexpression despite highly increased mRNA levels (2). We obtained similar data here with a vector coding HA-Pontin, and found that inhibition of proteasome enhanced the stability of newly synthesized Pontin and allowed a higher accumulation of Pontin (Fig. 7C-D). This gives support to the hypothesis that the lack of high-level protein expression is explained by a degradation of the newly translated protein that cannot find its binding partner.

A co-depletion of proteins engaged in functional complexes has been already shown for instance in the case of the Ku70–Ku80 heterodimer (31) or the γ -secretase complex (32). However, in no case were full mechanistic data provided. In addition, our findings are unique in that we show that destabilization of the protein partner intervenes at an early post-translational stage.

From our findings, one would expect that the depletion of either protein would result in the same cellular phenotype. This is indeed what was observed in our experiments when comparing depletion of Reptin (2) and Pontin (this study) on cell growth and apoptosis, and also by others on the formation of RAD51 nuclear foci after DNA damage in prostate cancer cells (11). In the yeast, genome-wide microarray analysis after acute deletion of either protein showed a striking correlation between the genes regulated by each protein (6). More generally, knockdown, inactivation or deletion of either gene in *Drosophila* (10) or yeast (33) resulted in a similarly lethal phenotype. These data have been interpreted as Pontin and Reptin having non-redundant functions. We suggest that they could be re-interpreted on the basis of the co-depletion of both proteins. Still, it is likely that Pontin and Reptin have some unique functions as suggested by several observations. Indeed, whereas Pontin depletion with siRNAs led to spindle defects in *Drosophila* S2 and HeLa cells, Reptin siRNAs had no effect (34). Pontin and Reptin also antagonistically modulate β -catenin transcriptional activity (10, 14, 16, 22), likely because they are incorporated into different complexes and differentially recruited onto target promoters (9, 35). These apparently unique functions may be due to a small pool of Pontin and Reptin not engaged in heteromeric complexes but present as monomers of homo-oligomers. Although structural studies suggest mostly hetero-complex formation (17, 18), they do not exclude the possibility of other forms (18).

In summary, Pontin, like Reptin, is overexpressed in HCC and is required for HCC growth and viability. We demonstrate that the expression of both proteins is strictly co-regulated by a post-translational mechanism involving the proteasomal degradation of newly synthesized proteins. We also found that Pontin and Reptin expression are highly correlated at the mRNA level in HCC thus suggesting some additional co-regulation at the mRNA level. Altogether, the whole data indicate the importance to maintain a strict control of the stoichiometry between Pontin and Reptin for proper cell homeostasis and likely for their role in carcinogenesis.

Acknowledgements:

Grant support : The work was supported by grants from Agence Nationale pour la Recherche sur le SIDA et les Hépatites Virales, Institut National du Cancer (PL06_117), Association pour la Recherche sur le Cancer (4026), Ligue Nationale Contre le Cancer and Conseil Régional d'Aquitaine. VH was the recipient of a fellowship from Agence Nationale pour la Recherche sur le SIDA et les Hépatites Virales, and AN from Institut National du Cancer.

We thank Pierre Laurent-Puig (Paris, France) for help with statistical analysis, Otmar Huber (Berlin, Germany) for antibodies, Michael Cole (Lebanon, NH, USA) and Irina Tsaneva (London, UK) for plasmids, Harald Wodrich (Bordeaux, France) for ubiquitin tools and know-how, and Marc Piechaczyk (Montpellier, France) for helpful discussions.

Abbreviations

HCC : Hepatocellular carcinoma

AAA+ : ATPases associated with various cellular activities

References:

1. Blanc J, Lalanne C, Plomion C, Schmitter J, Bathany K, Gion J. Proteomic analysis of differentially expressed proteins in hepatocellular carcinoma developed in patients with chronic viral hepatitis C. *Proteomics*. 2005; 5 : 3778 - 3789
2. Rousseau B, Menard L, Haurie V, Taras D, Blanc JF, Moreau-Gaudry F. Overexpression and role of the ATPase and putative DNA helicase RuvB-like 2 in human hepatocellular carcinoma. *Hepatology*. 2007; 46 : 1108 - 1118
3. Hanson PI, Whiteheart SW. AAA+ proteins: have engine, will work. *Nat Rev Mol Cell Biol*. 2005; 6 : 519 - 529
4. Gallant P. Control of transcription by Pontin and Reptin. *Trends Cell Biol*. 2007; 17 : 187 - 192
5. Huber O, Menard L, Haurie V, Nicou A, Taras D, Rosenbaum J. Pontin and reptin, two related ATPases with multiple roles in cancer. *Cancer Res*. 2008; 68 : 6873 - 6876
6. Jonsson ZO, Dhar SK, Narlikar GJ, Auty R, Wagle N, Pellman D. Rvb1p and Rvb2p are essential components of a chromatin remodeling complex that regulates transcription of over 5% of yeast genes. *J Biol Chem*. 2001; 276 : 16279 - 16288
7. Ikura T, Ogryzko VV, Grigoriev M, Groisman R, Wang J, Horikoshi M. Involvement of the TIP60 histone acetylase complex in DNA repair and apoptosis. *Cell*. 2000; 102 : 463 - 473
8. Shen X, Mizuguchi G, Hamiche A, Wu C. A chromatin remodelling complex involved in transcription and DNA processing. *Nature*. 2000; 406 : 541 - 544
9. Kim JH, Kim B, Cai L, Choi HJ, Ohgi KA, Tran C. Transcriptional regulation of a metastasis suppressor gene by Tip60 and beta-catenin complexes. *Nature*. 2005; 434 : 921 - 926
10. Bauer A, Chauvet S, Huber O, Usseglio F, Rothbacher U, Aragnol D. Pontin52 and reptin52 function as antagonistic regulators of beta-catenin signalling activity. *Embo J*. 2000; 19 : 6121 - 6130
11. Gospodinov A, Tsaneva I, Anachkova B. RAD51 foci formation in response to DNA damage is modulated by TIP49. *Int J Biochem Cell Biol*. 2009; 41 : 925 - 933
12. King TH, Decatur WA, Bertrand E, Maxwell ES, Fournier MJ. A well-connected and conserved nucleoplasmic helicase is required for production of box C/D and H/ACA snoRNAs and localization of snoRNP proteins. *Mol Cell Biol*. 2001; 21 : 7731 - 7746
13. Venteicher AS, Meng Z, Mason PJ, Veenstra TD, Artandi SE. Identification of ATPases pontin and reptin as telomerase components essential for holoenzyme assembly. *Cell*. 2008; 132 : 945 - 957
14. Bauer A, Huber O, Kemler R. Pontin52, an interaction partner of beta-catenin, binds to the TATA box binding protein. *Proc Natl Acad Sci U S A*. 1998; 95 : 14787 - 14792

- 15 . Kanemaki M , Makino Y , Yoshida T , Kishimoto T , Koga A , Yamamoto K . Molecular cloning of a rat 49-kDa TBP-interacting protein (TIP49) that is highly homologous to the bacterial RuvB . *Biochem Biophys Res Commun* . 1997 ; 235 : 64 - 68
- 16 . Wood MA , McMahon SB , Cole MD . An ATPase/helicase complex is an essential cofactor for oncogenic transformation by c-Myc . *Mol Cell* . 2000 ; 5 : 321 - 330
- 17 . Puri T , Wendler P , Sigala B , Saibil H , Tsaneva IR . Dodecameric structure and ATPase activity of the human TIP48/TIP49 complex . *J Mol Biol* . 2007 ; 366 : 179 - 192
- 18 . Torreira E , Jha S , Lopez-Blanco JR , Arias-Palomo E , Chacon P , Canas C . Architecture of the pontin/reptin complex, essential in the assembly of several macromolecular complexes . *Structure* . 2008 ; 16 : 1511 - 1520
- 19 . Zhao R , Davey M , Hsu YC , Kaplanek P , Tong A , Parsons AB . Navigating the chaperone network: an integrative map of physical and genetic interactions mediated by the hsp90 chaperone . *Cell* . 2005 ; 120 : 715 - 727
- 20 . Bioulac-Sage P , Rebouissou S , Sa Cunha A , Jeannot E , Lepreux S , Blanc JF . Clinical, morphologic, and molecular features defining so-called telangiectatic focal nodular hyperplasias of the liver . *Gastroenterology* . 2005 ; 128 : 1211 - 1218
- 21 . Livak KJ , Schmittgen TD . Analysis of relative gene expression data using real-time quantitative PCR and the 2(-Delta Delta C(T)) Method . *Methods* . 2001 ; 25 : 402 - 408
- 22 . Weiske J , Huber O . The histidine triad protein Hint1 interacts with Pontin and Reptin and inhibits TCF-beta-catenin-mediated transcription . *J Cell Sci* . 2005 ; 118 : 3117 - 3129
- 23 . Neaud V , Gillibert Duplantier J , Mazzocco C , Kisiel W , Rosenbaum J . Thrombin Up-regulates Tissue Factor Pathway Inhibitor-2 Synthesis through a Cyclooxygenase-2-dependent, Epidermal Growth Factor Receptor-independent Mechanism . *J Biol Chem* . 2004 ; 279 : 5200 - 5206
- 24 . Bastide A , Karaa Z , Bornes S , Hieblot C , Lacazette E , Prats H , Touriol C . An upstream open reading frame within an IRES controls expression of a specific VEGF-A isoform . *Nucleic Acids Res* . 2008 ; 36 : 2434 - 2445
- 25 . Aberle H , Bauer A , Stappert J , Kispert A , Kemler R . beta-catenin is a target for the ubiquitin-proteasome pathway . *Embo J* . 1997 ; 16 : 3797 - 3804
- 26 . Te J , Jia L , Rogers J , Miller A , Hartson SD . Novel subunits of the mammalian Hsp90 signal transduction chaperone . *J Proteome Res* . 2007 ; 6 : 1963 - 1973
- 27 . Zhao R , Kakahara Y , Gribun A , Huen J , Yang G , Khanna M . Molecular chaperone Hsp90 stabilizes Pih1/Nop17 to maintain R2TP complex activity that regulates snoRNA accumulation . *J Cell Biol* . 2008 ; 180 : 563 - 578
- 28 . Jonsson ZO , Jha S , Wohlschlegel JA , Dutta A . Rvb1p/Rvb2p recruit Arp5p and assemble a functional Ino80 chromatin remodeling complex . *Mol Cell* . 2004 ; 16 : 465 - 477
- 29 . Glickman MH , Ciechanover A . The ubiquitin-proteasome proteolytic pathway: destruction for the sake of construction . *Physiol Rev* . 2002 ; 82 : 373 - 428
- 30 . Jariel-Encontre I , Bossis G , Piechaczyk M . Ubiquitin-independent degradation of proteins by the proteasome . *Biochim Biophys Acta* . 2008 ; 1786 : 153 - 177
- 31 . Nussenzweig A , Chen C , da Costa Soares V , Sanchez M , Sokol K , Nussenzweig MC , Li GC . Requirement for Ku80 in growth and immunoglobulin V(D)J recombination . *Nature* . 1996 ; 382 : 551 - 555
- 32 . Edbauer D , Winkler E , Haass C , Steiner H . Presenilin and nicastrin regulate each other and determine amyloid beta-peptide production via complex formation . *Proc Natl Acad Sci U S A* . 2002 ; 99 : 8666 - 8671
- 33 . Kanemaki M , Kurokawa Y , Matsu-ura T , Makino Y , Masani A , Okazaki K . TIP49b, a new RuvB-like DNA helicase, is included in a complex together with another RuvB-like DNA helicase, TIP49a . *J Biol Chem* . 1999 ; 274 : 22437 - 22444
- 34 . Ducat D , Kawaguchi S , Liu H , Yates JR 3rd , Zheng Y . Regulation of Microtubule Assembly and Organization in Mitosis by the AAA+ ATPase Pontin . *Mol Biol Cell* . 2008 ; 19 : 3097 - 3110
- 35 . Diop SB , Bertaux K , Vasanthi D , Sarkeshik A , Goirand B , Aragnol D . Reptin and Pontin function antagonistically with PcG and TrxG complexes to mediate Hox gene control . *EMBO Rep* . 2008 ; 9 : 260 - 266
- 36 . Chevet E , Wong HN , Gerber D , Cochet C , Fazel A , Cameron PH . Phosphorylation by CK2 and MAPK enhances calnexin association with ribosomes . *Embo J* . 1999 ; 18 : 3655 - 3666

Figure 1

Expression of Pontin in human hepatocellular carcinoma

(A) Pontin mRNA levels were measured with real-time RT-PCR in 104 HCC and 18 non-tumoral livers (NT). Gene expression results were normalized to internal control ribosomal 18S. The graph shows the mean \pm 1 SD of mRNA levels. (B) Correlations between Pontin and Reptin mRNA levels in HCC and non-tumor (NT) samples. (C) Pontin immunostaining at the junction between the HCC (left) and the surrounding non-tumoral liver that is separated from the tumor by a fibrous capsule. Staining appears as a brown color. The inset shows a consecutive section stained with a control IgG. (D) Reptin immunostaining on a consecutive section. (E) Pontin immunostaining on a high-power view of the tumor where an intense cytoplasmic staining is detectable. (F) Disease-free survival (DFS) curves according to Pontin mRNA levels. Log-rank test comparison of low versus high levels gave a P value at 0.0022.

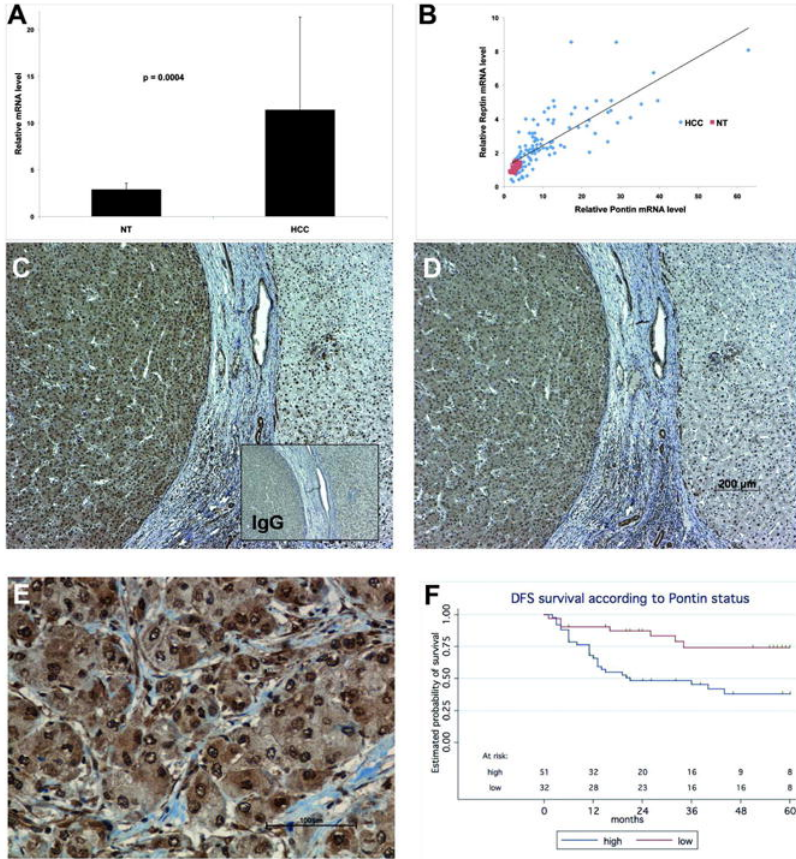


Figure 2

Efficiency and effects of silencing of Pontin by siRNAs in HuH7 cells

(A) Relative expression of Pontin mRNA in HuH7 24h post-transfection of Pontin siRNA (P1 and P2) or control siRNA (scP). Gene expression was measured by real-time RT-PCR. Results are normalized on the basis of the expression of GAPDH and on the level of the non-transfected cells (NT). The graph shows the mean \pm 1 SD of 3 independent experiments. (B) Western blot showing Pontin expression 3 days after siRNA transfection in HuH7. The same blot was re-hybridized with a β -actin antibody. (C) Cell proliferation was measured at indicated times after siRNAs transfection. Shown are the means \pm 1 SEM of 3 experiments conducted in duplicate. Proliferation of P1 and P2 transfected cells was significantly different in comparison with controls (NT and scP) ($p < 0.001$). (D) BrdU incorporation and caspase 3 activity measured in cells after transfection of siRNA against Pontin (P1 and P2) or scrambled P2 duplexes (scP). Values are means \pm 1 SD of three experiments. BrdU incorporation was significantly reduced and caspase-3 activity increased in P1 and in P2 transfected cells compared to scrambled-transfected cells ($p < 0.001$ and $p < 0.05$, respectively).

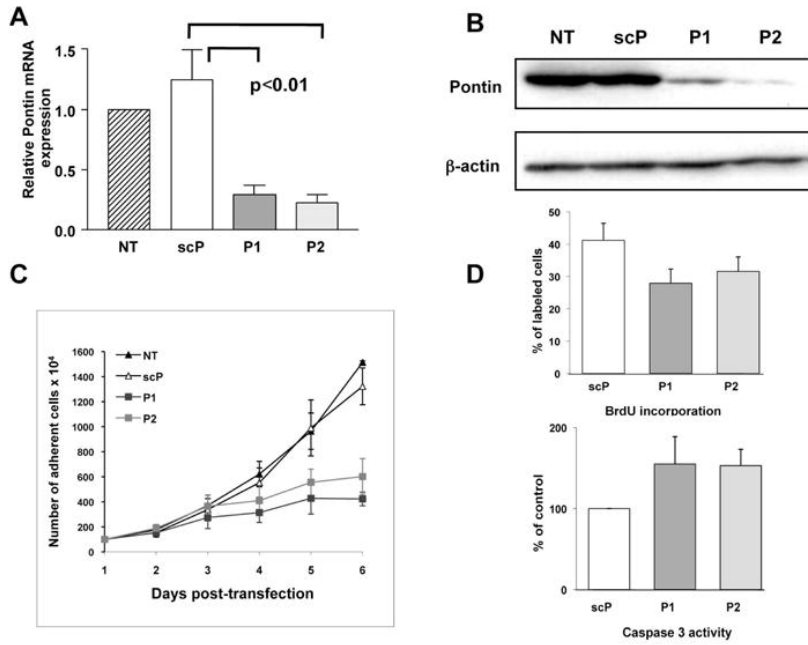


Figure 3

Silencing of Reptin or Pontin by specific siRNAs leads to down-regulation of both proteins

(A) Western blot of Pontin and Reptin expression in HuH7 cells three days after transfection of siRNAs targeting Reptin (R1 and R2), Pontin (P1 and P2) or Luciferase (GL2). (B) The graph shows the relative amounts of Pontin and Reptin. All values are the mean \pm 1SD of at least 3 independent experiments. (C) HuH7 cells expressing HA-Pontin (wt) or HA-Pontin resistant to P2 siRNA (res) were transfected with control (GL2) or Pontin siRNAs (P1 or P2). Expression of Pontin and Reptin was analyzed by western blot. In cells expressing HA-Pontin resistant to P2, Reptin level was not decreased after transfection of P2. In contrast, P1 siRNA depleted together Pontin, HA-Pontin and Reptin (note that HA-Pontin cannot be distinguished from endogenous Pontin on these gels). (D) HuH7 cells expressing Flag-Reptin resistant to R2 siRNA were transfected with control (GL2) or Reptin siRNAs (R1 or R2). In cells expressing Flag-Reptin resistant to R2, the level of Pontin was not decreased after transfection of R2. In contrast, R1 siRNA depleted together Reptin, Flag-Reptin and Pontin. The arrow indicates the upper band revealed with the anti-Reptin antibody, corresponding to Flag-Reptin.

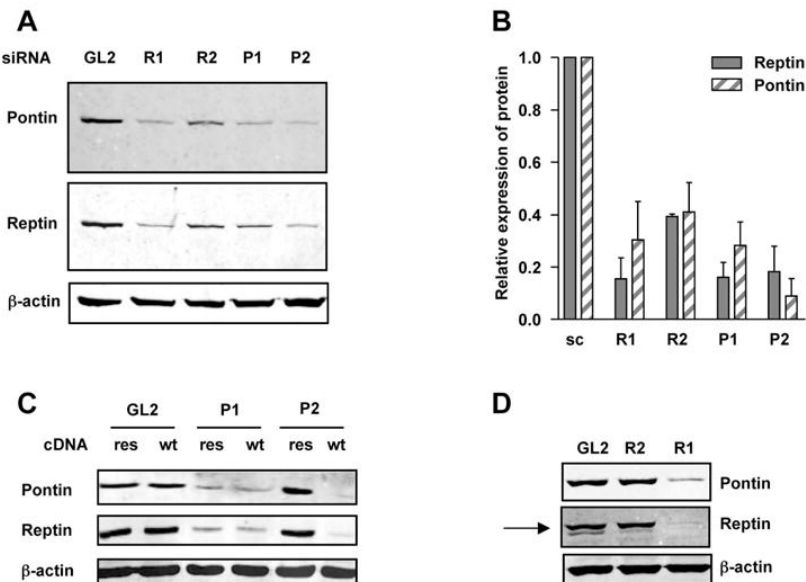
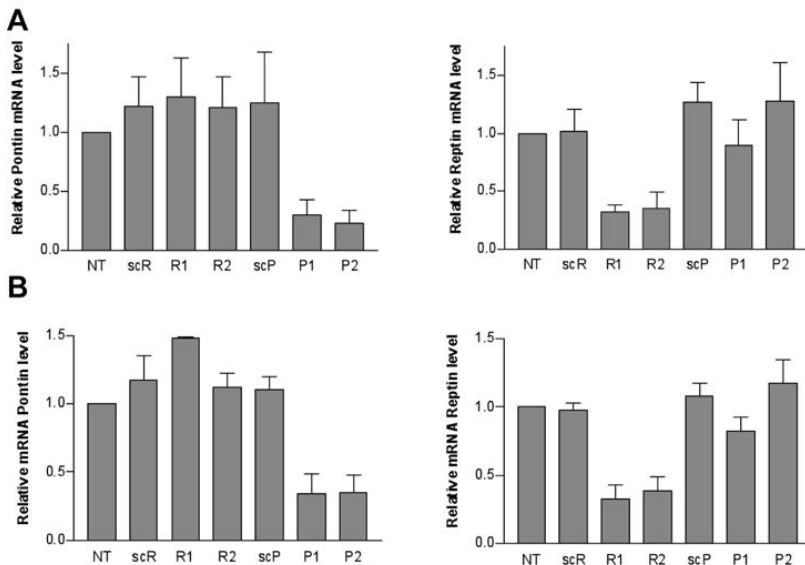


Figure 4

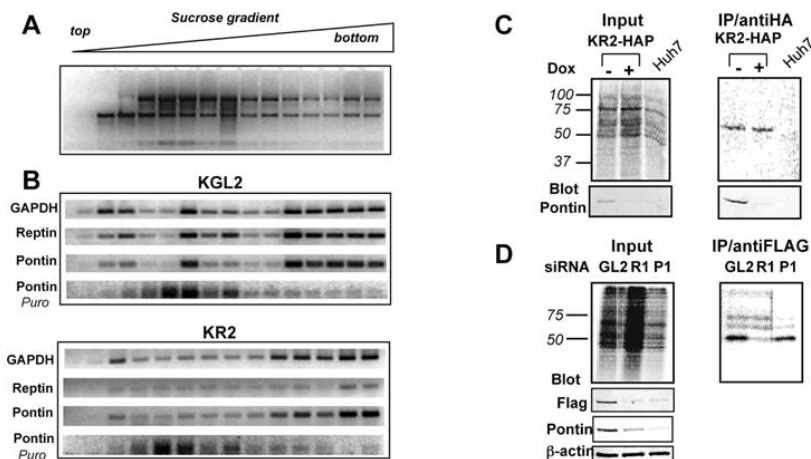
Expression of Reptin and Pontin transcripts following silencing

(A) Total RNA was purified 24h after transfection of Pontin (P1 and P2) or Reptin specific siRNAs (R1 and R2). Scrambled P2 (scP) or R2 (scR) duplexes were used as controls. RNAs were used for RT-qPCR analysis of Pontin (left) or Reptin (right) mRNAs. The results are expressed as relative expression of Reptin and Pontin normalized to GAPDH and are the mean \pm 1SD of at least three independent experiments. Pontin and Reptin mRNAs were significantly decreased only following transfection of their targeting siRNAs ($p < 0.001$ by ANOVA). (B) Same experiment performed 48 h after transfection of siRNAs.

**Figure 5**

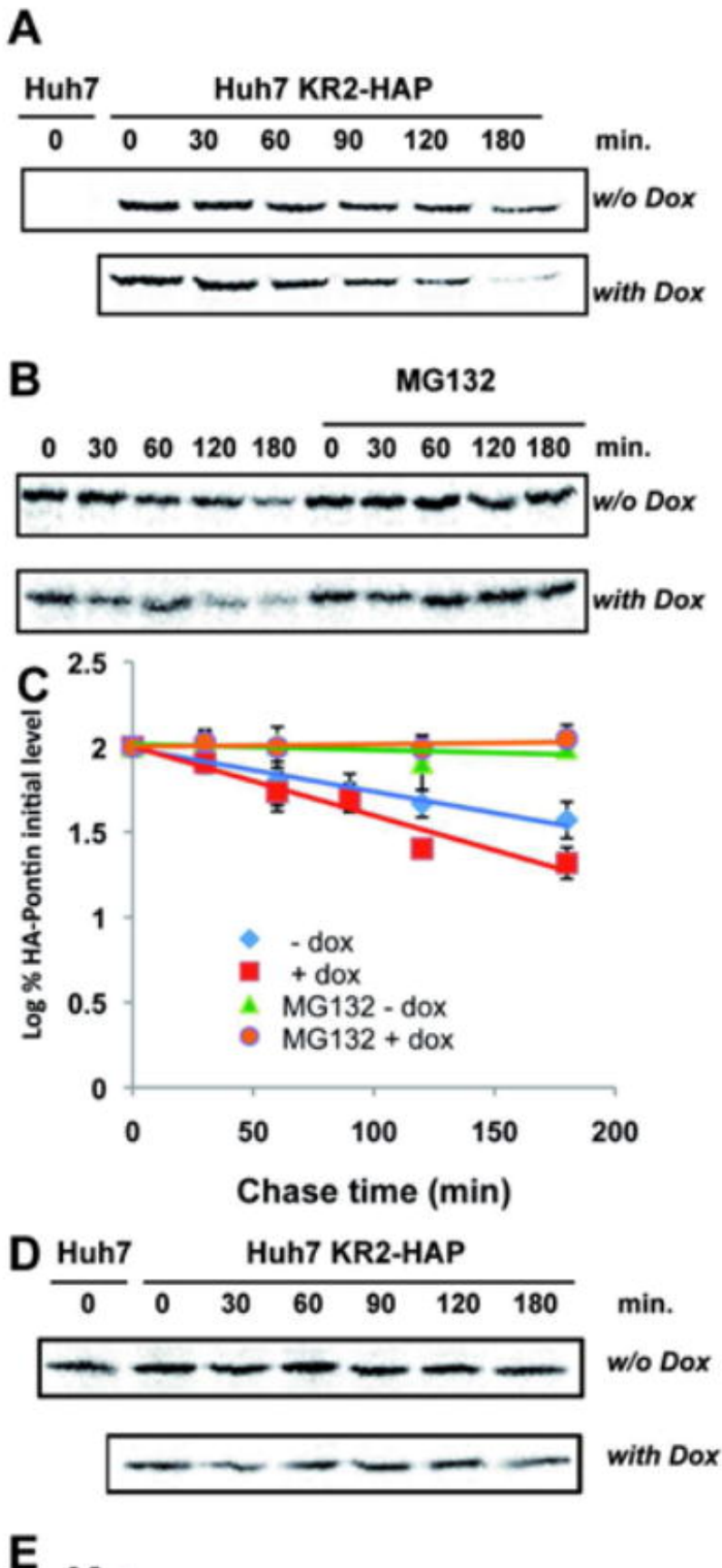
Distribution of Reptin and Pontin mRNA in polysomes, and translation of Pontin

(A) Representative distribution of ribosomal RNAs in a sucrose gradient visualized by ethidium bromide staining. RNA from each fraction was analyzed by RT-PCR. (B) Distribution of GAPDH, Reptin and Pontin mRNA in polysomes. KGL2 or KR2 cells that stably express a doxycycline-inducible shRNA against luciferase or Reptin, respectively, were grown with or without 0.02 μ g/ml doxycycline for 3 days before cell fractionation. Polysome profile analyses were carried out 3 times, with similar results. (C) Normal translation of Pontin in Reptin-depleted cells. Cells were grown for 4 days with or without doxycycline, then pulsed for 15 min with [35 S] methionine/cysteine. The overall profile of newly synthesized proteins is not altered upon Reptin depletion (top left panel). Depletion of Pontin in KR2-HAP treated with doxycycline was shown by immunoblotting with an anti-Pontin antibody (bottom left). HA-pontin was immunoprecipitated with anti-HA antibody. Signals from immunoprecipitated radiolabeled polypeptides were acquired with an Instant-Imager (top right). The identity of the labeled band was confirmed by immunodetection with an anti-Pontin antibody (bottom right). As a control, no labeled polypeptide was immunoprecipitated with anti-HA in extracts from wild type HuH7 cells. (D) Normal translation of Flag-Reptin in Pontin-depleted cells. Cells were grown for 5 days after transfection of control (GL2), Reptin (R1) or Pontin (P1) siRNAs, then pulsed for 15 min with [35 S] methionine/cysteine. The overall profile of newly synthesized proteins is not altered upon Reptin or Pontin depletion (top left panel). Depletion of Pontin and Flag-Reptin in Huh7 cells after transfection of R1 and P1 siRNAs was shown by immunoblotting with anti-FLAG and anti-Pontin antibodies (bottom left). FLAG-Reptin was immunoprecipitated with anti-FLAG antibody. Signals from immunoprecipitated radiolabeled polypeptides were acquired with an Instant-Imager (top right).

**Figure 6**

Half-life of Pontin

(A) Pulse-chase analysis of HA-tagged Pontin in KR2-HAP cells in Reptin-replete ("w/o dox") or Reptin-depleted conditions ("with dox"). Equal amounts of cell lysates were immunoprecipitated with an anti-HA antibody. Eluates were loaded onto a SDS-PAGE. As a control, no labeled polypeptide was immunoprecipitated with anti-HA in extracts from wild type HuH7 cells (lane 1). (B) Same experiment except that the chase medium was supplemented or not with the proteasome inhibitor MG132 (25 μ M). (C) The graph shows relative quantitation of radiolabeled protein from at least 3 independent experiments. Counts from t0 were arbitrarily set at 100%. (D) Pulse-chase analysis of Calnexin half-life. Calnexin was immunoprecipitated from the flow-through fractions after centrifugation of anti-HA-agarose bead, using a rabbit polyclonal anti-Calnexin antibody (36), followed by protein A-Sepharose beads. (E) Graphical analysis of (D) following signal quantitation.



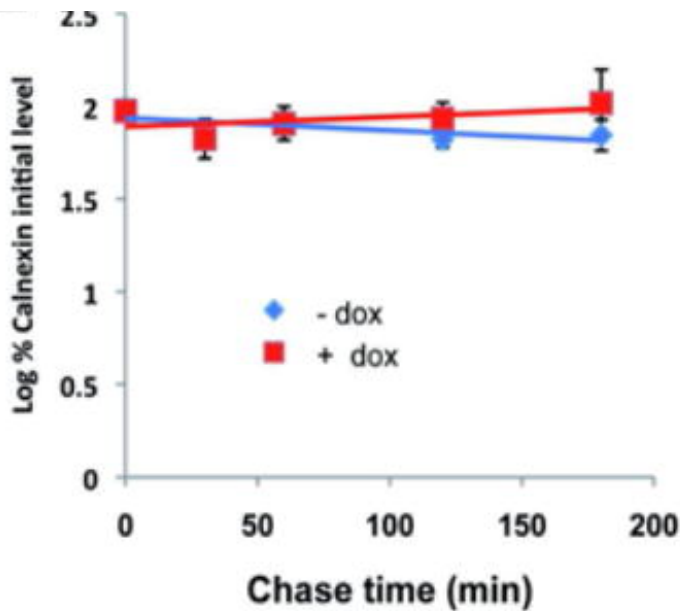


Figure 7

Effect of proteasome inhibitors on the decrease in Pontin levels upon Reptin depletion

(A) Western blot of Reptin and Pontin expression in KR2 cells. After three days with or without doxycyclin, cells were treated with 25 μ M MG132, 2.5 μ M epoxomycin, or DMSO during 4 hours. The same samples were also analyzed for β -catenin expression. (B) Expression of Pontin in KR2-HAP cells. Left, cells were pulse-labeled and Pontin was immunoprecipitated. The top panel shows newly synthesized Pontin, and the bottom one total Pontin. There was a 4.9 fold increase in newly synthesized Pontin in cells expressing HA-Pontin as compared to control cells. On the right side, Western blot for Pontin. Pontin level was increased by only 1.2 fold in KR2 HAP cells as compared to control cells. (C) After 3 days of culture with or without doxycycline, cells were treated for 4h with 25 μ M MG132 or DMSO. Cell extracts were subjected to Western blot with the indicated antibodies. (D) Quantification of experiments shown in (C) (n = 3). (E) Treatment with cycloheximide prevents the restoration by MG132 of Pontin levels in Reptin-depleted cells. Cells were treated as in (C). In some cases (cycloheximide (CHX, 50 μ M) was added at the same time than MG132. (F) Same as in (E) except that epoxomycin was used instead of MG132.

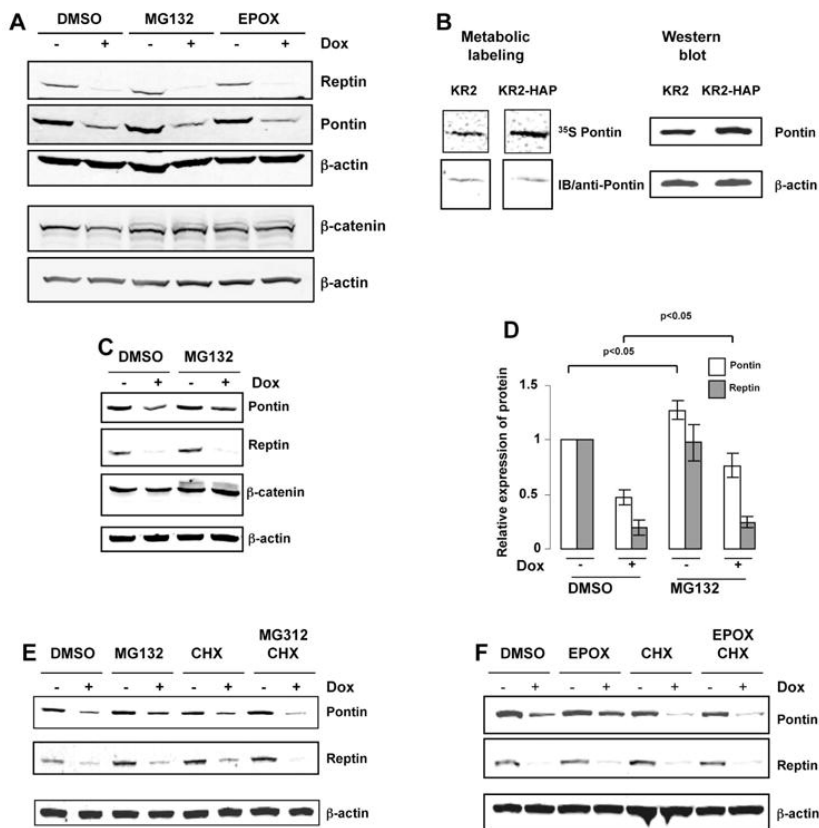


Figure 8

Evidence for the involvement of ubiquitylation in the destabilization of Pontin and Reptin

(A–B) Effect of proteasome and ubiquitin-activating enzyme inhibitors on the stability of newly-synthesized Pontin. HuH7 cells expressing the inducible R2 Reptin shRNA together with HA-Pontin (KR2-HAP) were treated or not with Dox for 3 days. Metabolic labelling and immunoprecipitation were as in Fig. 6 . The chase period was 180 min and was done in the presence of 25 μ M MG132, 50 μ M UBEI-41 (Ubel) or DMSO (CTRL). (A) Overall pattern of radiolabeled neosynthesized proteins (top) and western blots for Pontin, Reptin and β -actin in the cell extract (bottom). (B) Detection of newly-synthesized HA-Pontin following immunoprecipitation with the HA antibody (top); the bottom part shows the quantification of two independent experiments. (C–D) Effect of proteasome and ubiquitin-activating enzyme inhibitors on the stability of newly-synthesized Reptin. HuH7 cells expressing the inducible P2 Pontin shRNA together with Flag-Pontin (KP2-FR) were treated as above, except that immunoprecipitation was carried out with the Flag antibody. (C) Overall pattern of radiolabeled neosynthesized proteins (top) and western blots for Reptin, Pontin and β -actin in the cell extract (bottom). (D) Detection of newly-synthesized Flag-Reptin following immunoprecipitation with the Flag antibody Note that all lanes from the IP experiment come from the same gel and were exposed simultaneously.

